Neutron diffraction studies of the magnetoelastic compounds Tb$_5$Si$_x$Ge$_{4-x}$ (x=2.2 and 2.5)

V. O. Garlea,[1,*] J. L. Zarestky,[1] C. Y. Jones,[2] L.-L. Lin,[1] D. L. Schlagel,[3] T. A. Lograsso,[3] A. O. Tsokol,[3] V. K. Pecharsky,[3,4] K. A. Gschneidner, Jr.,[3,4] and C. Stassis[1]

[1]*Ames Laboratory and Department of Physics, Iowa State University, Ames, Iowa 50011, USA*
[2]*National Institute of Standards and Technology, Gaithersburg, Maryland 20899, USA*
[3]*Materials and Engineering Physics Program, Ames Laboratory, Ames, Iowa 50011, USA*
[4]*Department of Materials Science and Engineering, Iowa State University, Ames, Iowa 50011, USA*

We report the results of a neutron diffraction study, carried out on both single crystalline and polycrystalline samples of Tb$_5$Si$_{2.2}$Ge$_{1.8}$ and polycrystalline Tb$_5$Si$_{2.5}$Ge$_{1.5}$. On cooling, at approximately 120 K, the Tb$_5$Si$_{2.2}$Ge$_{1.8}$ system undergoes a magnetoelastic transition from a high-temperature monoclinic-paramagnetic to a low-temperature orthorhombic-ferromagnetic structure. Between 120 K and 75 K, the magnetic structure has a net ferromagnetic component along the a axis direction. The moments are slightly canted with respect to the a axis, while the components along the b and c axes are ordered antiferromagnetically. A second magnetic transition occurs at approximately 75 K. Below this temperature, the magnetic structure consists of ferromagnetically aligned μ_x and μ_z projections of the magnetic moments and an antiferromagnetic arrangement of the μ_y moment components. Magnetic structures of Tb$_5$Si$_{2.5}$Ge$_{1.5}$ are nearly identical to those of Tb$_5$Si$_{2.2}$Ge$_{1.8}$.

I. INTRODUCTION

Systematic research performed over the last decade reveals that the family of R_5Si$_x$Ge$_{4-x}$ pseudobinary alloys, where R is a rare earth metal, exhibit some startling magnetoresponsive properties associated both with their layered crystal structures and the combined magnetic-martensitic transformations below room temperature.[1–5] These include the giant magnetocaloric effect, colossal magnetostriction, and giant magnetoresistence.

The crystal structures of compounds in R_5Si$_x$Ge$_{4-x}$ systems can be described as the stacking of identical, well-defined blocks of atoms (i.e., the slabs) $[R_5T_4]^\infty$, where T = Si or Ge atoms, perpendicular to the b axis (see Fig. 1). These slabs consist of rare earth atoms, the majority of which are located in the corners of slightly distorted cubes and trigonal prisms, and a small fraction inside the cubes. Each R atom inside the cube is octahedrally coordinated with six T atoms; four of these T atoms are located inside the slab and two are positioned on the opposite surfaces of the slabs, playing a crucial role in the interslab bonding.[5] The interslab interactions and, consequently, the crystal and magnetic sublattices of many R_5Si$_x$Ge$_{4-x}$ compounds exhibit extreme sensitivity to any or all of the following thermodynamic variables: chemical composition [both the nature of the R-component and the concentration of the Si(Ge) atoms, x],[6,7] temperature,[8] pressure,[9] and magnetic field.[10,11]

To date, only a few studies dedicated to the determination of the magnetic and structural phase diagrams of the Tb$_5$Si$_x$Ge$_{4-x}$ series have been reported.[11–17] Over the range of composition $1.6 < x < 2.8$, the room temperature crystal structure of the R_5Si$_x$Ge$_{4-x}$ compounds is a monoclinically distorted variant of the well-known Sm$_5$Ge$_4$-type[18] structure. The monoclinic lattice is composed of alternating strongly and weakly interacting slabs,[12,13] in effect, creating a peculiar sequence of weakly interacting pairs of slabs which was

originally postulated for the Gd$_5$Si$_2$Ge$_2$ compound.[7,8] This crystal structure is displayed in Fig. 1. Macroscopic measurements indicate that a paramagnetic to ferromagnetic phase transition occurs in Tb$_5$Si$_x$Ge$_{4-x}$ alloys below room temperature, and that Curie temperature varies from $\sim$170 K to $\sim$80 K as the concentration of Si is reduced from $x \cong 2.8$ to $x \cong 1.6$. This disorder-order transformation is followed by a second magnetic phase transition associated with a spin reorientation at lower temperatures. Ritter *et al.*[13] used neutron powder diffraction to characterize some of the magnetic phases in the Tb$_5$Si$_x$Ge$_{4-x}$ system and established that when $1.6 < x < 2.8$, the high-temperature magnetic ordering is accompanied by a martensitic like transformation from a monoclinic Gd$_5$Si$_2$Ge$_2$-type to an orthorhombic Gd$_5$Si$_4$-type[7] structure. In the latter, strong interaction between all of the slabs is reestablished. In the monoclinic structure, a total of
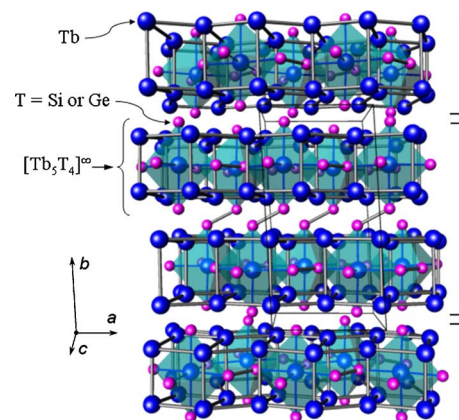

FIG. 1. (Color online) Perspective view of the room temperature crystal structure of the Tb$_5$Si$_x$Ge$_{4-x}$ compounds with $1.6 < x < 2.8$ along the c axis. Bracket on the left highlights one of the $[R_5T_4]^\infty$ slabs. Square brackets on the right indicate pairs of strongly interacting slabs.

20 Tb atoms per unit cell are distributed among five general $4e$ sites in the space group $P112_1/a$, while in the orthorhombic structure, the same 20 Tb atoms of the $Tb_5Si_xGe_{4-x}$ intermetallic compounds are located in two general $8d$ and one special $4c$ sites of the space group $Pnma$, thus the number of positional degrees of freedom among the R atoms varies from 15 to 8 independent variables. More recently, Morellon *et al.*[11] discovered a monoclinic-ferromagnetic phase in the compound with $x=2$ and demonstrated that the structural and magnetic transformations on cooling at ambient pressure are separated by approximately 10 K. They both can be made to occur at approximately 115 K by applying a hydrostatic pressure between 8 and 9 kbar.[11]

Progress in understanding the properties of these compounds has been hindered by difficulties in growing large, high-quality single crystals. Recently a single crystal of $Tb_5Si_{2.2}Ge_{1.8}$ was grown at the Ames Laboratory and this motivated us to initiate a neutron diffraction study of this compound as a function of temperature. Here, we report a detailed analysis of the magnetomartensitic transformation, performed on two different $Tb_5Si_xGe_{4-x}$ stoichiometries, i.e., with $x=2.2$ and 2.5, using both single-crystal and powder neutron diffraction measurements. The use of single-crystal neutron diffraction techniques allows in most cases the determination of directions of the magnetic moments.

II. EXPERIMENTAL DETAILS

A single crystal with $Tb_5Si_{2.2}Ge_{1.8}$ stoichiometry was grown at the Ames Laboratory using the tri-arc assisted crystal pulling method as described elsewhere,[19] starting from a polycrystalline raw material. The polycrystalline alloys with $x=2.2$ and 2.5 were prepared by arc melting in an argon atmosphere from high-purity constituent elements weighed according to the target stoichiometries. The given alloy was remelted six times to ensure its homogeneity. The samples were characterized by means of x-ray diffraction (backscatter Laue for the single crystals and powder technique for the polycrystals), magnetic susceptibility, and specific heat measurements. No impurity phases were detected by x-ray diffraction at room temperature. The residual resistivity ratio of the single crystal is highly anisotropic: $\rho(300K)/\rho(4.2K)$ $=6.4$ when measured along the b axis and it is close to 1 when measured along the a axis. Due to the increase of the temperature-independent component of the resistivity as the result of magnetostructural transition around 110 K, the residual resistivity measurements were not conclusive in indicating the samples' purity.[4]

The single-crystal elastic neutron scattering measurements were performed on the Ames Laboratory's fixed-incident energy triple-axis spectrometer, HB1A, located at the High Flux Isotope Reactor (HFIR) at the Oak Ridge National Laboratory (ORNL). The HB1A spectrometer operates with a fixed initial energy of 14.7 meV using a double pyrolitic graphite (PG) monochromator system, a PG analyzer, and two PG filters located before and after the second monochromator. As a result, the second-order contamination of the beam incident on the sample is negligible (i.e., $I_{\lambda/2} \cong 10^{-4}I_\lambda$) and the higher order contaminations are substantially re-duced. Collimations of $48'$-$40'$-$40'$-$136'$ were used. Measurements were performed on two single-crystal samples with dimensions of 2.5 mm diameter×7 mm height and 3.5 mm diameter×7.5 mm height. The quality of crystals was checked by performing rocking curve measurements. The mosaic spread of the crystals at $(0k0)$-type reflections was found to be approximately 0.5° (full width at half maximum) and about 0.4° at $(h00)$ reflections, which is broader than our experimental resolution. Estimates indicate negligible extinction in the samples. For the low-temperature study, the crystals were placed inside an aluminum can filled with helium exchange gas and mounted on a cold finger of a closed cycle refrigerator.

Neutron powder diffraction measurements were carried out using the BT-1 high-resolution neutron powder diffractometer at the NIST Center for Neutron Research (NCNR). It is a 32 detector instrument that can be used with three different monochromators and two different incident Soller collimators, allowing the instrument response to be tailored to the needs of the experiment. Our measurements were performed using an in-pile collimation of $15'$ and a Cu(311) monochromator which has a takeoff angle of 90° reflecting neutrons with wavelength 1.5402(2)Å. Data were collected over the range of $3° < 2\theta < 165°$ with a 2θ step size of 0.05°. A more detailed description of the BT-1 instrument can be found elsewhere.[20]

III. EXPERIMENTAL RESULTS AND DISCUSSION

A. Single-crystal elastic neutron scattering study

Single-crystal elastic neutron scattering measurements were performed over the 8–300 K temperature range, on two different single crystals of composition $Tb_5Si_{2.2}Ge_{1.8}$, successively oriented such that the a-b, a-c, and b-c planes coincide with the horizontal scattering plane. In Fig. 2, we show selected neutron elastic scans along the a^*, b^*, and c^* reciprocal space directions at 130 K, 75 K, and 10 K. Above approximately 120 K, only the nuclear reflections consistent with the monoclinic crystal structure (shown in Fig. 1) are observed. As the temperature decreases below ~120 K, a phase transition from a monoclinic to an orthorhombic structure accompanied by an ordering of the magnetic moments is detected. These observations are in good agreement with the room temperature x-ray and the temperature-dependent macroscopic measurements, results of which will be published elsewhere. There is indeed a peak in the ac magnetic susceptibility curve (not shown here), clearly indicating magnetic ordering at 120 K. Furthermore, macroscopic measurements indicate that at this temperature, $Tb_5Si_{2.2}Ge_{1.8}$ exhibits a giant magnetocaloric effect peaking at approximately 37 J/kg K for a magnetic field change of 50 kOe. Figure 2 shows the appearance of the magnetic contributions to the nuclear reflections as well as additional magnetic peaks forbidden in the crystallographic space group $Pnma$ [allowed reflections are $(h00)$ where $h=2n$; $(0k0)$, $k=2n$; $(00l)$, $l=2n$, $(hk0)$, $h=2n$; $(0kl)$, $k+l=2n$]. No intermediate magnetic-only transformation of the monoclinic phase has been detected in the vicinity of 120 K. If there is a difference
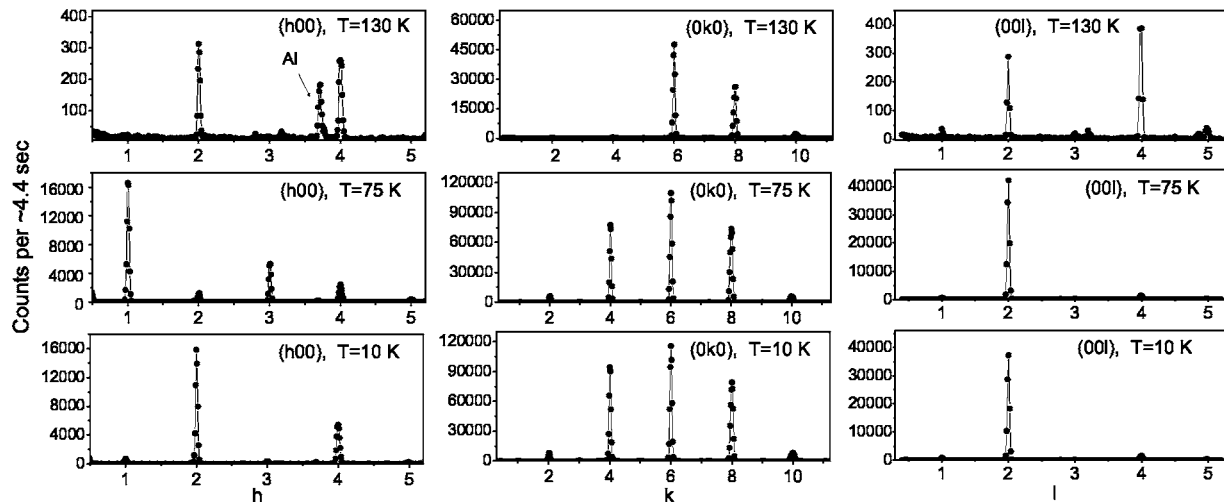
FIG. 2. Typical elastic scans along [$h00$], [$0k0$], and [$00l$] directions at 130 K, 75 K, and 10 K. These scans were performed in two different scattering planes: ($00l$) and ($h00$). The measured intensities were normalized to the intensities of ($0k0$) reflections. Data collected at 130 K were indexed in a monoclinic cell ($\gamma \approx 93°$) while at 75 K and 10 K in an orthorhombic cell.

in the magnetic and martensitic transition temperature, as observed in $Tb_5Si_2Ge_2$,[11] then it is smaller than the 5-K temperature step used in our experiment.

The evolution in temperature of the integrated intensities of selected reflections is presented in Fig. 3. In particular, below approximately 120 K a rapid increase of intensities of purely magnetic ($h=2n+1, 0, 0$)-type reflections is observed. These reflections attain a maximum intensity at approximately 75 K and then decrease rapidly with decreasing temperature. In contrast, the ($h=2n, 0, 0$) reflections exhibit at 120 K a slight increase in intensity caused by the modification of the crystal structure. They remain constant, within

FIG. 3. (Color online) Evolution in temperature of integrated intensities of (100), (200), (002), and (040) reflections.

experimental error, down to approximately 75 K, suggesting that no additional magnetic intensity is superimposed over these nuclear reflections. As the temperature is lowered below 75 K, the ($h=2n, 0, 0$) peak intensities increase as the temperature decreases and show a tendency towards saturation at approximately 25 K. On the other hand, the order parameter curves below 75 K show a slight decrease of the intensity of the reflections measured along the c^* direction ($0, 0, l=2n$) but a monotonic increase of the ($0, k=2n, 0$) intensities with decreasing temperature. These findings point to a change in symmetry of the magnetic order at approximately 75 K, which is consistent with the results of macroscopic measurements showing a second magnetic transition at approximately 70 K for $x=2.2$. The order parameter curves measured during cooling and heating show a hysteresis of approximately 7 K around the first transition temperature (at ∼120 K). No hysteresis has been detected around the second transition (at ∼75 K).

In order to generate all possible magnetic structures that are compatible with the crystal structure, we have employed the representation analysis technique,[21] using the program SARAH.[22] There are eight possible irreducible representations associated with the $Pmna$ space group.[17] In the temperature range 120 K to 75 K, the magnetic structure can be well described using a single irreducible representation (Γ_3) corresponding to the Shubnikov magnetic space group $Pnm'a'$. This confirms the magnetic model employed by Ritter *et al.*,[13] in fitting their neutron powder diffraction data of $Tb_5Si_2Ge_2$ collected at 100 K and 85 K. The basis functions of the irreducible representation Γ_3 are listed in Table I. Group theoretical considerations indicate that the Γ_3 representation is described by the F_x and C_z magnetic modes for the Tb atoms located at $4c$ site and, respectively, the $F_{Bx}A_{By}G_{Bz}$ modes at $8d$ sites. These modes are specified by the relative signs of the μ_x, μ_y, or μ_z magnetic moment components of each of the $4c$ or $8d$ positions within the chemical cell: $F_x(++++)$, $C_z(++--)$, $F_{Bx}(++++++++)$, $A_{By}(+--++--+)$, and $G_{Bz}(+-+-+-+-)$. This implies that the projections of the magnetic moments along the a axis
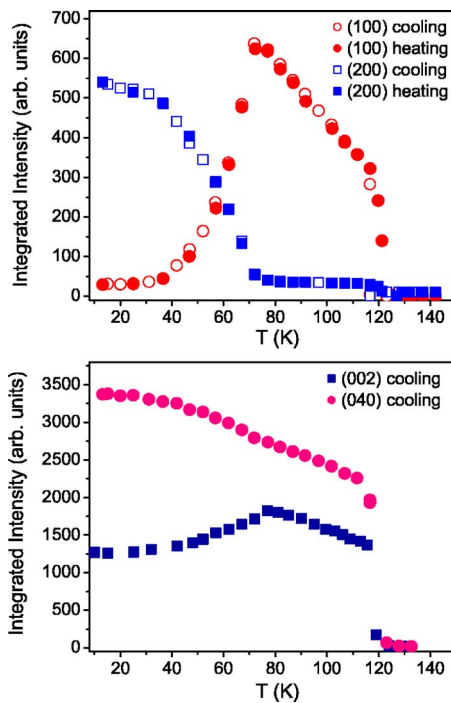
TABLE I. The basis functions of the irreducible representations Γ_3 and Γ_7 of the space group *Pnma* ($\vec{k}=0$).

Atom position	$\Gamma_3(Pnm'a')$			$\Gamma_7(Pn'm'a)$		
4c	F_x		C_z	C_x		F_z
$x, \frac{1}{4}, z$	(100)		(001)	(100)		(001)
$-x, \frac{3}{4}, -z$	(100)		(001)	(100)		(001)
$\frac{1}{2}-x, \frac{3}{4}, \frac{1}{2}+z$	(100)		$(00\bar{1})$	$(\bar{1}00)$		(001)
$\frac{1}{2}+x, \frac{1}{4}, \frac{1}{2}-z$	(100)		$(00\bar{1})$	$(\bar{1}00)$		(001)
8d	F_{Bx}	A_{By}	G_{Bz}	G_{Bx}	C_{By}	F_{Bz}
x, y, z	(100)	(010)	(001)	(100)	(010)	(001)
$\frac{1}{2}+x, \frac{1}{2}-y, \frac{1}{2}-z$	(100)	$(0\bar{1}0)$	$(00\bar{1})$	$(\bar{1}00)$	(010)	(001)
$-x, \frac{1}{2}+y, -z$	(100)	$(0\bar{1}0)$	(001)	(100)	$(0\bar{1}0)$	(001)
$\frac{1}{2}-x, -y, \frac{1}{2}+z$	(100)	(010)	$(00\bar{1})$	$(\bar{1}00)$	$(0\bar{1}0)$	(001)
$-x, -y, -z$	(100)	(010)	(001)	(100)	(010)	(001)
$\frac{1}{2}-x, \frac{1}{2}+y, \frac{1}{2}+z$	(100)	$(0\bar{1}0)$	$(00\bar{1})$	$(\bar{1}00)$	(010)	(001)
$x, \frac{1}{2}-y, z$	(100)	$(0\bar{1}0)$	(001)	(100)	$(0\bar{1}0)$	(001)
$\frac{1}{2}+x, y, \frac{1}{2}-z$	(100)	(010)	$(00\bar{1})$	$(\bar{1}00)$	$(0\bar{1}0)$	(001)

(μ_x) order ferromagnetically and those along the *b* axis and the *c* axis (μ_y and μ_z, respectively) order antiferromagnetically. The magnetic point group of the Tb 4c site is m' which leads to a magnetic moment lying in the mirror plane whose normal is collinear with the *b* axis.

Since the neutrons sense only the projection of the magnetic moments in the plane perpendicular to the scattering vector, the rapid increase of the magnetic contribution to the nuclear reflections measured along the a^* direction below approximately 75 K can be associated with a development of ferromagnetic coupling perpendicular to the *a* axis. Moreover, the decreasing peak intensities measured along the c^* direction, with decreasing temperature below 75 K (see Fig. 3), indicate an increase of the component of the moment along the *c* axis (μ_z). The less dramatic monotonic increase of the $(0, k=2n, 0)$ intensities indicates that there is no notable change in the μ_y components and the magnetic moments remain almost confined to the *a-c* plane. The only irreducible representation associated with *Pnma* space group that holds the antisymmetry mirror plane m' and yields a ferromagnetic component perpendicular to the *a* axis is Γ_7, which corresponds to the Shubnikov group $Pn'm'a$ (also shown in Table I). However, this representation does not allow the ferromagnetic ordering of the μ_x components. As a consequence, below 75 K, the magnetic structure can only be described using the basis vectors of two different irreducible representations Γ_3 and Γ_7 and consist of a ferromagnetic alignment of the μ_x and μ_z components ($F_x F_z$ modes) and an antiferromagnetic coupling of the μ_y components. Unfortunately, a unique determination of the antiferromagnetic sequence for the components parallel to the *b* axis was not possible, given the limited data set collected with the triple-axis spectrometer and the possibility of several models of magnetic structure with similar structure factors. To formu-

late magnetic structure models for temperatures below 75 K, the single-crystal study was supplemented with neutron powder diffraction measurements.

B. Powder diffraction measurements

Neutron powder diffraction measurements were performed at various temperatures for two different compositions: $Tb_5Si_{2.2}Ge_{1.8}$ and $Tb_5Si_{2.5}Ge_{1.5}$. Measurements were made on approximately 37 g of a sample held in a vanadium can with length 5.08 cm and 1.57 cm diameter. Rietveld refinements were carried out using the FULLPROF program.[23]

The refinements of neutron diffraction patterns recorded in the paramagnetic state at room temperature confirmed that $Tb_5Si_xGe_{4-x}$ crystallize in a monoclinic structure with the $P112_1/a$ space group when $x=2.2$ and $x=2.5$. In the refinement, the fractional occupancies of the *T*-atoms sites were fixed to the values required by the sample stoichiometry assuming a completely statistical mixing of the Si and Ge atoms; and the atoms with the same atomic number were constrained to have identical thermal displacement parameters. The atomic coordinates and the lattice parameters resulting from the fits are listed in Table II. Upon cooling the $Tb_5Si_{2.2}Ge_{1.8}$ sample, we observed two low $Q(=4\pi \sin \theta/\lambda)$ weak magnetic reflections appearing at approximately 85 K ($Q \approx 0.42$ Å^{-1}) and 50 K ($Q \approx 0.46$ Å^{-1}). We have identified these peaks as corresponding to the strongest magnetic reflections of Tb_5Si_3 and Tb_5Ge_3 phases, whose intensities are roughly an order of magnitude larger than those of the strongest nuclear reflections.[24,25] The two impurity peaks were excluded from all refinements.

As a next step, refinements of the nuclear and magnetic structures were performed using diffraction patterns recorded at 100 K and 75 K. At these temperatures, both $Tb_5Si_{2.2}Ge_{1.8}$

TABLE II. Results of the structure refinement of $Tb_5Si_xGe_{4-x}$, $x=2.2$ and $x=2.5$, at room temperature.

$T=298$ K	$Tb_5Si_{2.2}Ge_{1.8}$				$Tb_5Si_{2.5}Ge_{1.5}$			
Atom	x	y	z	B_{iso}(Å)	x	y	z	B_{iso}(Å)
Tb1($4e$)	0.326(1)	0.2466(5)	0.0027(9)	0.74(1)	0.325(1)	0.2474(6)	0.005(1)	0.86(1)
Tb2($4e$)	−0.0040(9)	0.0982(4)	0.1867(8)	0.74(1)	−0.005(1)	0.0985(6)	0.181(1)	0.86(1)
Tb3($4e$)	0.0178(8)	0.4012(4)	0.179(1)	0.74(1)	0.015(1)	0.4015(5)	0.179(1)	0.86(1)
Tb4($4e$)	0.3570(9)	0.8814(4)	0.1670(9)	0.74(1)	0.358(1)	0.8824(5)	0.169(1)	0.86(1)
Tb5($4e$)	0.3308(8)	0.6215(4)	0.1714(8)	0.74(1)	0.3314(9)	0.6216(5)	0.174(1)	0.86(1)
Si1/Ge1($4e$)	0.950(1)	0.2498(6)	0.895(1)	0.94(1)	0.950(1)	0.2493(7)	0.895(1)	1.02(1)
Si2/Ge2($4e$)	0.205(1)	0.2500(6)	0.368(1)	0.94(1)	0.206(2)	0.2484(6)	0.365(1)	1.02(1)
Si3/Ge3($4e$)	0.205(1)	0.9559(7)	0.463(1)	0.94(1)	0.207(1)	0.9580(6)	0.468(1)	1.02(1)
Si4/Ge4($4e$)	0.153(1)	0.5400(6)	0.470(1)	0.94(1)	0.158(1)	0.5397(7)	0.467(1)	1.02(1)
Lattice cell and reliability factors	$a=7.5181(3)$Å, $b=14.6767(3)$Å, $c=7.7153(1)$Å, $\gamma=93.110(4)°$, $V_{cell}=850.07(8)$Å^3, $R_{Bragg}=4.27\%$, $R_p=3.08\%$, $R_{wp}=3.9\%$, $\chi^2=1.14$				$a=7.5142(4)$Å, $b=14.6715(9)$Å, $c=7.7110(5)$Å, $\gamma=93.094(5)°$, $V_{cell}=848.8(1)$Å^3, $R_{Bragg}=4.62\%$, $R_p=2.78\%$, $R_{wp}=3.5\%$, $\chi^2=1.26$			

and $Tb_5Si_{2.5}Ge_{1.5}$ crystallize in the orthorhombic Gd_5Si_4-type structure with the space group *Pnma*. As shown in the previous section, above approximately 75 K, the neutron diffraction data were best fit with a magnetic structure described by the magnetic modes F_xC_z at the $4c$ site and $F_{Bx}A_{By}G_{Bz}$ at $8d$ positions, of the irreducible representation Γ_3 (Shubnikov space group *Pnm'a'*).

As indicated by the single crystal analysis, below approximately 75 K, the magnetic structure consists of the ferromagnetic alignment of the μ_x and μ_z projections of the magnetic moments, described, respectively, by F_x and F_z magnetic modes, at each of the Tb positions. On the other hand, the projections parallel to the b axis order antiferromagnetically and several sequences of the moment orientations had to be successively tested. A satisfactory fit of neutron powder data was obtained using the sequences: $C_{By}(++--++--)$ of $\Gamma_7(Pn'm'a)$ representation at the Tb2($8d$) position and $A_{By}(+-++--+)$ of the $\Gamma_3(Pnm'a')$ representation at the Tb3($8d$) position. However, the magnetic structure that gives the best agreement with experimental data, among all allowed models, was described using the basis vectors of two irreducible representations (Γ_2,Γ_4) associated with a different space group symmetry, $P2_12_12_1$, which is a subgroup of the *Pnma* space group. The two irreducible representations Γ_2 and Γ_4 correspond to the Shubnikov space groups $P2_12_1'2_1'$ and $P2_1'2_1'2_1$. Nevertheless, neither of these refinements allows an unambiguous choice between the two models; the obtained reliability factors being close to each other (e.g., for $Tb_5Si_{2.2}Ge_{1.8}$, $R_{mag}=6.3\%$ in the case of the first model and $R_{mag}=5.5\%$ for the second one).

In the second model, the Tb atoms in $8d$ sites of the *Pnma* space group split into two $4a$ positions ($P2_12_12_1$) but the magnitude of the magnetic moments were constrained to remain the same. The magnetic ordering along the b axis was described using the coupling $C_y\bar{A}_y(++---++-)$ and $C_yA_y(++--+--+)$ at the Tb2 and Tb3 position respectively.

Ritter *et al.*[13] described their low-temperature data for $Tb_5Si_2Ge_2$ using a magnetic model where the orientation of the magnetic moments approximately agrees with our first model using the basis vectors of Γ_3 and Γ_7. The difference is in the fact that Ritter *et al.*[13] split the set of magnetic Tb ions in $4c$ and $8d$ sites into two subsets and refine them independently, allowing a different magnitude of the magnetic mo-
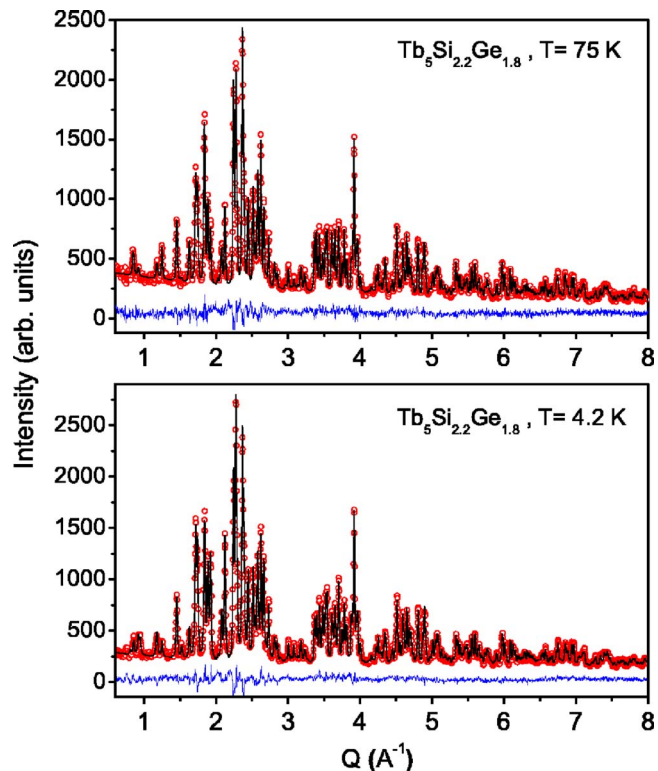

FIG. 4. (Color online) Observed neutron diffraction pattern (circles), calculated profile (solid line) and their difference (bottom line) for $Tb_5Si_{2.2}Ge_{1.8}$ at $T=75$ K and 4 K.

TABLE III. Results of the Rietveld refinement of $Tb_5Si_xGe_{4-x}$, $x=2.2$ and $x=2.5$, at $T=75$ K and 4.2 K.

Atom	T (K)	$Tb_5Si_{2.2}Ge_{1.8}$				$Tb_5Si_{2.5}Ge_{1.5}$			
		x	y	z	B_{iso} (Å)	x	y	z	B_{iso} (Å)
Tb1(4c)	75	0.3488(6)	1/4	−0.0092(4)	0.21(2)	0.3504(6)	1/4	−0.0092(4)	0.35(2)
	4.2	0.3490(5)	1/4	−0.0086(4)	0.17(2)	0.3489(5)	1/4	−0.0085(4)	0.27(2)
Tb2(8d)	75	0.0246(4)	0.0965(1)	0.8174(3)	0.21(2)	0.0255(4)	0.0967(1)	0.8177(3)	0.35(2)
	4.2	0.0234(3)	0.0965(1)	0.8183(3)	0.17(2)	0.0233(3)	0.0967(1)	0.8181(3)	0.27(2)
Tb3(8d)	75	0.1791(4)	0.1229(1)	0.3224(0)	0.21(2)	0.1797(4)	0.1230(1)	0.3211(3)	0.35(2)
	4.2	0.1805(3)	0.1234(1)	0.3219(3)	0.17(2)	0.1815(3)	0.1231(1)	0.3210(3)	0.27(2)
Si1/Ge1(4c)	75	0.981(1)	1/4	0.093(1)	0.80(7)	0.980(1)	1/4	0.093(1)	0.63(7)
	4.2	0.983(1)	1/4	0.092(1)	0.52(6)	0.983(1)	1/4	0.092(1)	0.48(8)
Si2/Ge2(4c)	75	0.226(1)	1/4	0.631(1)	0.80(7)	0.227(1)	1/4	0.632(1)	0.63(7)
	4.2	0.229(1)	1/4	0.632(1)	0.52(6)	0.228(1)	1/4	0.632(1)	0.48(8)
Si3/Ge3(8d)	75	0.153(1)	0.9584(4)	0.526(1)	0.80(7)	0.153(1)	0.9568(5)	0.525(1)	0.63(7)
	4.2	0.1553(9)	0.9582(4)	0.5235(9)	0.52(6)	0.154(1)	0.9569(5)	0.524(1)	0.48(8)
Lattice cell and reliability factors	75	$a=7.4344(3)$Å, $b=14.6389(6)$Å, $c=7.7138(3)$Å, $V_{cell}=839.50$ Å^3, $R_{Bragg}=6.3\%$, $R_{mag}=5.5\%$, $R_p=5.0\%$, $R_{wp}=6.4\%$, $\chi^2=1.4$				$a=7.4337(4)$Å, $b=14.6377(4)$Å, $c=7.7093(4)$Å, $V_{cell}=838.86$ Å^3, $R_{Bragg}=6.1\%$, $R_{mag}=5.7\%$, $R_p=4.6\%$, $R_{wp}=5.9\%$, $\chi^2=1.55$			
	4.2	$a=7.4344(3)$Å, $b=14.6372(6)$Å, $c=7.7056(3)$Å, $V_{cell}=838.52$ Å^3, $R_{Bragg}=6.1\%$, $R_{mag}=5.5\%$, $R_p=4.7\%$, $R_{wp}=6.0\%$, $\chi^2=2.45$				$a=7.4355(3)$Å, $b=14.6368(7)$Å, $c=7.7014(4)$Å, $V_{cell}=838.15$ Å^3, $R_{Bragg}=4.7\%$, $R_{mag}=4.7\%$, $R_p=4.2\%$, $R_{wp}=5.5\%$, $\chi^2=2.66$			

TABLE IV. Magnetic structural data obtained from the Rietveld refinement using powder diffraction data recorded at 100 K, 75 K, 40 K, and 4.2 K.

	T(K)	$Tb_5Si_{2.2}Ge_{1.8}$				$Tb_5Si_{2.5}Ge_{1.5}$			
		μ_x (μ_B)	μ_y (μ_B)	μ_z (μ_B)	$\langle\mu\rangle$ (μ_B)	μ_x (μ_B)	μ_y (μ_B)	μ_z (μ_B)	$\langle\mu\rangle$ (μ_B)
Tb1(4c)	100	8.3(1)	0	0.47(7)	8.3(1)	8.2(1)	0	0.05(8)	8.2(1)
	75	8.5(1)	0	0.2(1)	8.5(1)	8.7(1)	0	0.4(1)	8.7(1)
	40[a]	8.2(1)	0	5.0(1)	9.6(1)	8.2(1)	0	4.6(1)	9.4(1)
	40[b]	8.0(1)	0	5.2(1)	9.5(1)	7.8(1)	0	5.1(1)	9.3(1)
	4.2[a]	8.2(1)	0	5.2(1)	9.7(1)	8.2(1)	0	5.4(1)	9.8(1)
	4.2[b]	7.8(1)	0	5.6(1)	9.6(1)	7.9(1)	0	5.7(1)	9.7(1)
Tb2(8d)	100	6.87(7)	2.18(1)	1.42(7)	7.3(1)	7.03(9)	1.72(9)	1.08(8)	7.3(1)
	75	7.30(7)	1.92(8)	1.77(6)	7.7(1)	7.58(8)	1.84(8)	1.52(6)	7.9(1)
	40[a]	6.73(8)	2.03(8)	5.98(6)	9.2(1)	6.8(1)	1.92(7)	5.3(1)	8.8(1)
	40[b]	6.7(1)	2.9(1)	6.0(1)	9.4(1)	6.95(9)	2.4(1)	5.4(1)	9.1(1)
	4.2[a]	6.26(8)	2.27(5)	6.18(9)	9.1(1)	6.86(9)	2.1(1)	5.95(9)	9.2(1)
	4.2[b]	6.42(8)	3.26(7)	6.30(9)	9.5(1)	6.96(8)	2.99(8)	6.13(9)	9.6(1)
Tb3(8d)	100	7.44(9)	0.4(1)	0.4(1)	7.4(1)	7.24(9)	0.1(1)	0.2(1)	7.2(1)
	75	7.91(9)	0.27(9)	0.34(9)	7.9(1)	8.01(9)	0.17(9)	0.53(8)	8.1(1)
	40[a]	8.38(1)	2.2(1)	3.7(1)	9.3(1)	7.9(1)	2.06(9)	3.2(1)	8.7(1)
	40[b]	8.2(1)	1.4(1)	3.9(1)	9.2(1)	8.0(1)	1.7(1)	3.4(1)	8.8(1)
	4.2[a]	7.95(9)	2.13(8)	4.28(9)	9.2(1)	8.5(1)	2.27(8)	3.60(9)	9.5(1)
	4.2[b]	7.93(8)	1.2(1)	4.53(8)	9.2(1)	8.45(9)	1.5(1)	3.92(8)	9.4(1)

[a]Model 1.
[b]Model 2.
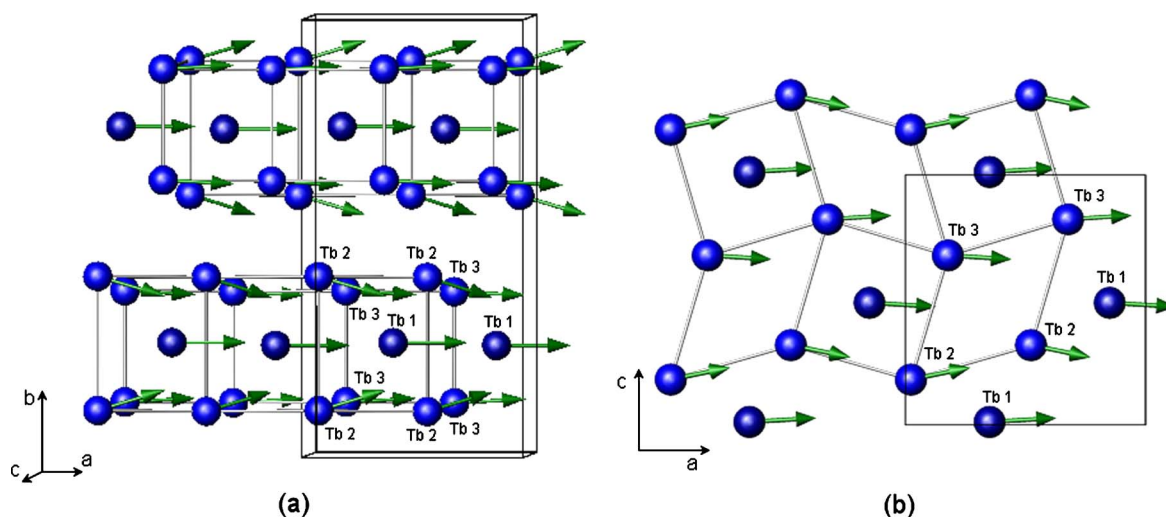
FIG. 5. (Color online) (a) Graphical representation of the orthorhombic-ferromagnetic structure of $Tb_5Si_{2.2}Ge_{1.8}$ in the temperature range 75 K $<$ T $<$ 120 K. The nonmagnetic atoms (Si/Ge) were excluded for clarity. (b) Projection of the magnetic structure on the a-c plane. The projection shows the Tb2, Tb3 atoms contained in one layer, and the Tb1 atoms located between the layers; all these atoms have the same orientation of the μ_y moment component.

ment at each subset. Figure 4 displays our experimental diffraction patterns and calculated profiles for the $Tb_5Si_{2.2}Ge_{1.8}$ sample at 75 K and 4 K, respectively. The refinement results, including structural and magnetic data for the two studied $Tb_5Si_xGe_{4-x}$ compounds, are summarized in Tables III and IV.

C. Description of the magnetic structure models

We have confirmed that at approximately 120 K, the $Tb_5Si_{2.2}Ge_{1.8}$ compound undergoes a magnetoelastic transformation from a monoclinic-paramagnetic to an orthorhombic-ferromagnetic structure. Analysis of the neutron diffraction data collected at temperatures above 75 K leads to a magnetic structure with a net ferromagnetic component. The moments are slightly canted with respect to the a axis, while the components along the b and c axes are antiferromagnetically ordered. In the case of $Tb_5Si_{2.2}Ge_{1.8}$, at 75 K, the Tb1, Tb2, and Tb3 canting angles with respect to the a axis are 1.3°, 19.6°, and 3.1°, respectively. It is worth noting that the interatomic distances between Tb2 atoms from neighboring slabs are much larger than the distances between Tb3 atoms belonging to different slabs, i.e., $d_{Tb2-Tb2} \cong 4.49$ Å and $d_{Tb3-Tb3} \cong 3.72$ Å. The shortest bonds correspond to the interslab contacts Tb2-Tb3, ($d_{Tb2-Tb3} \cong 3.71$ Å).

As shown in Fig. 5(a), above 75 K, there is an antiferromagnetic Tb2-Tb2 or Tb3-Tb3 coupling between the layers of Tb atoms that belong to the same slab and a ferromagnetic Tb3-Tb2 coupling between the slabs. It is likely that the intraslab coupling between the Tb atoms is through an indirect Ruderman-Kittel-Kasuya-Yosida (RKKY) 4f-4f exchange interaction, but it is also believed that the long-range ferromagnetic order exists only as long as all slabs are connected together enabling the Tb-Si(Ge)-Tb superexchange interactions.[5,26] In the same slab [see Fig. 5(b)], the Tb2 and Tb3 atoms form two zigzag chains, coupled ferromagneti-

cally with respect to each other. Each of these undulating chains runs along the a axis and contains antiferromagnetically coupled μ_z moment components.

Both magnetic models proposed for low temperatures, below 75 K, consist of a ferromagnetic arrangement of all a- and c-axes magnetic moment components. The refinement results show an increase of the magnetic moment projection along the c axis, and consequently, the canting angles with respect to the a-axis direction increase. In the case of $Tb_5Si_{2.2}Ge_{1.8}$, at 4.2 K, they become $\sim$ 35.6°, $\sim$47.8°, and $\sim$30.5° for Tb1, Tb2, and Tb3, respectively. The magnetic moment components along the b axis remain antiferromagnetically aligned and no significant change in the magnitude has been observed. The two magnetic models employed to describe the magnetic structure at low temperatures are displayed in Fig. 6. A two-dimensional projection of the magnetic structure in the a-c plane is depicted in Fig. 7. For the sake of clarity we recall that model 1 was made using the basis vectors of two irreducible representations (IR) associated with the $Pnma$ space group, while in model 2 we employed the basis vectors of two IR's associated with $P2_12_12_1$, a subgroup of $Pnma$. In model 1, the Tb layers are made by two interacting chains of Tb2 and Tb3 atoms, the b-axis component (μ_y) of Tb2 moments being aligned antiparallel and those of Tb3 aligned parallel with respect to each other. That implies the existence of alternating antiferromagnetically and ferromagnetically coupled chains running along both the a and c directions. In addition to that, the second model also contains layers where the b-axis components (μ_y) of Tb2 moments align ferromagnetically and those of Tb3 align antiferromagnetically with respect to each other. These two types of layers of similar topologies, alternate along the b-axis direction. In both models, the interslab interactions between Tb2 and Tb3 magnetic moments are mixed: ferromagnetic and antiferromagnetic.

As resulted from the refinement of neutron diffraction data for low temperatures, the magnitudes of the magnetic
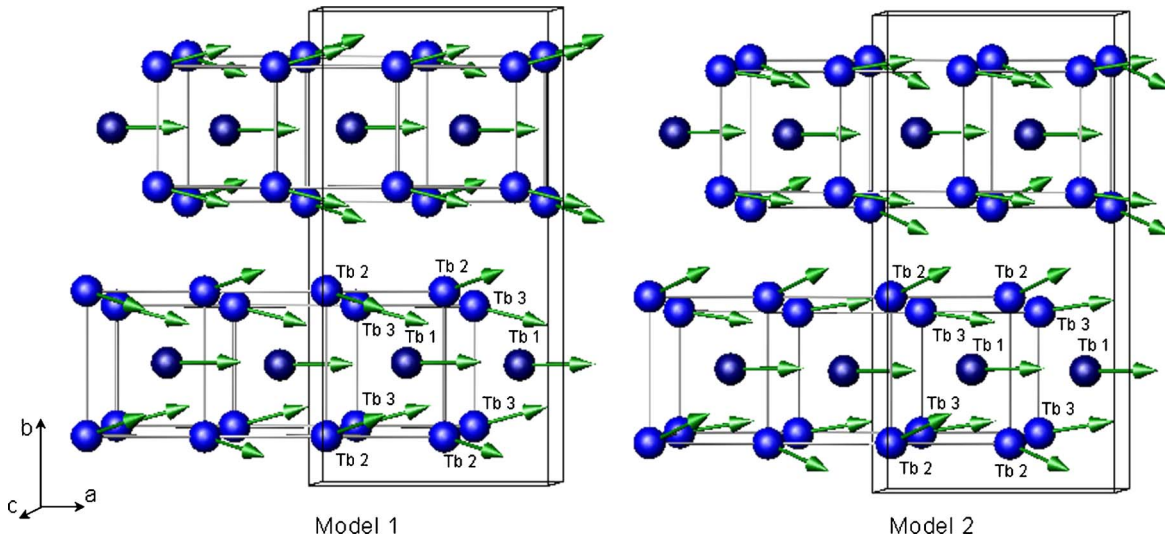
FIG. 6. (Color online) Two possible models of the magnetic structure of $Tb_5Si_{2.2}Ge_{1.8}$ below 75 K. Model 1 was described by mixing $Pnm'a'$ and $Pn'm'a$ while Model 2 using $P2_12_1'2_1'$ and $P2_1'2_1'2_1$. [The nonmagnetic atoms (Si/Ge) were excluded for clarity.]

moments of Tb atoms exceed the theoretically expected value of $gJ=9.0\ \mu_B$ assuming a purely $4f$-electron magnetism. Additional refinements were performed constraining individual components of the moments such that the total moment was limited to 9.0 μ_B. The magnetic reliability factor R_{mag} increases by 2%. Moreover, as can be seen in Table IV, this moment does not depend on the choice of the magnetic model. We note that Ritter *et al.*[13] also report magnetic moments of Tb atoms in Tb_5Si_4 and $Tb_5Si_2Ge_2$ considerably exceeding the expected 9.0 μ_B. Also, it is worth mentioning that the average spontaneous magnetic moments along the three principal crystallographic axes of $Tb_5Si_{2.2}Ge_{1.8}$, determined from the bulk magnetization measurements of a single crystal at 1.8 K (unpublished), are 7.7 μ_B, 2.5 μ_B, and 5.9 μ_B. Considering all of the errors involved, these values are quite close to the average weighed magnetic moments of 7.4 μ_B, 1.8 μ_B, and 5.5 μ_B along the same axes determined from the neutron data at 4.2 K. Thus, both techniques yield ordered magnetic moments of Tb atoms that exceed the

theoretical value, likely pointing to some contribution from the polarized $5d$-electrons of the Tb atoms. One must admit, however, that since most of the magnetic reflections are superposed with the nuclear reflections, the magnetic moments and the atomic displacement parameters are coupled and the real systematic errors could be larger than the statistical errors shown in parenthesis in the Table IV. It remains an open question as to why the Rietveld refinement results indicate such a large moment. Resolving this issue may require further experiments using polarized neutron scattering techniques.

IV. SUMMARY

We have studied the magnetic phase transitions of two $Tb_5Si_xGe_{4-x}$alloys, with $x=2.2$ and 2.5 by means of single-crystal and powder neutron diffraction techniques. We have confirmed that the large magnetocaloric effect in $Tb_5Si_xGe_{4-x}$ is related to a first-order phase transition between the high-temperature monoclinic-paramagnetic and the low temperature orthorhombic-ferromagnetic states of the material, which in $Tb_5Si_{2.2}Ge_{1.8}$ occurs at approximately 120 K. Between 120 K and 75 K, the measurements show a canted ferromagnetic structure with the a axis being the easy magnetization direction. Our measurements unambiguously indicate that a second magnetic transition occurs at approximately 75 K. Examination of the single-crystal data shows that the magnetic structure consists of a ferromagnetic alignment of the moment components parallel to the a and c axes. Two different models of the magnetic structure were used to describe an antiferromagnetic sequence of the moment components along the b axis in the low-temperature magnetically ordered state. A satisfactory fit of neutron powder data was obtained by mixing the basis vectors of two irreducible representations associated with $P2_12_12_1$, a subgroup of the *Pnma* space group.
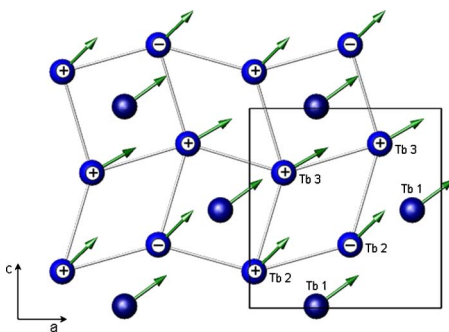

FIG. 7. (Color online) Projection of the magnetic structure of $Tb_5Si_{2.2}Ge_{1.8}$ on the a-c plane, below $T=75$ K. The figure shows the Tb2, Tb3 atoms contained in one layer, and the Tb1 atoms located between inside the slab; the magnetic components out of the plane are identified by $+(-)$ signs.

*Electronic address: garleao@ornl.gov

[1] V. K. Pecharsky and K. A. Gschneidner Jr., Phys. Rev. Lett. **78**, 4494 (1997).

[2] V. K. Pecharsky and K. A. Gschneidner Jr., Appl. Phys. Lett. **70**, 3299 (1997).

[3] L. Morellon, P. A. Algarabel, M. R. Ibarra, J. Blasco, B. Garcia Landa, Z. Arnold, and F. Albertini, Phys. Rev. B **58**, R14721 (1998).

[4] E. M. Levin, V. K. Pecharsky, and K. A. Gschneidner Jr., Phys. Rev. B **60**, 7993 (1999).

[5] V. K. Pecharsky and K. A. Gschneidner Jr., Adv. Mater. (Weinheim, Ger.) **13**, 683 (2001) and references therein.

[6] K. A. Gschneidner Jr., V. K. Pecharsky, A. O. Pecharsky, V. V. Ivtchenko, and E. M. Levin, J. Alloys Compd. **303&304**, 241 (2000).

[7] V. K. Pecharsky and K. A. Gschneidner Jr., J. Alloys Compd. **260**, 98 (1997).

[8] W. Choe, V. K. Pecharsky, A. O. Pecharsky, K. A. Gschneidner Jr., V. G. Young, Jr., and G. J. Miller, Phys. Rev. Lett. **84**, 4617 (2000).

[9] C. Magen, Z. Arnold, L. Morellon, Y. Skorokhod, P. A. Algarabel, M. R. Ibarra, and J. Kamarad, Phys. Rev. Lett. **91**, 207202 (2003).

[10] V. K. Pecharsky, A. P. Holm, K. A. Gschneidner Jr., and R. Rink, Phys. Rev. Lett. **91**, 197204 (2003).

[11] L. Morellon, C. Ritter, C. Magen, P. A. Algarabel, and M. R. Ibarra, Phys. Rev. B **68**, 024417 (2003); L. Morellon, Z. Arnold, C. Magen, C. Ritter, O. Prokhnenko, Y. Skorokhod, P. A. Algarabel, M. R. Ibarra, and J. Kamarad, Phys. Rev. Lett. **93**, 137201 (2004).

[12] H. Huang, A. O. Pecharsky, V. K. Pecharsky, and K. A. Gschneidner Jr., Adv. Cryog. Eng. **48**, 11 (2002).

[13] C. Ritter, L. Morellon, P. A. Algarabel, C. Magen, and M. R. Ibarra, Phys. Rev. B **65**, 094405 (2002).

[14] L. Morellon, C. Magen, P. A. Algarabel, M. R. Ibarra, and C. Ritter, Appl. Phys. Lett. **79**, 1318 (2001).

[15] N. P. Thuy, N. V. Nong, N. T. Hien, L. T. Tai, T. Q. Vinh, P. D. Thang, and E. Bruck, J. Magn. Magn. Mater. **242-245**, 841 (2002).

[16] A. Kupsch, A. A. Levin, and D. C. Meyer, Cryst. Res. Technol. **40**, 42 (2005).

[17] P. Schobinger-Papamantellos, J. Phys. Chem. Solids **39**, 197 (1978).

[18] G. S. Smith, Q. Johnson, and A. G. Tharp, Acta Crystallogr. **22**, 269 (1967).

[19] D. L. Schlagel, T. A. Lograsso, A. O. Pecharsky, and J. A. Sampaio, in *Light Metals 2005*, edited by Halvor Kvande (The Minerals, Metals & Materials Society, Warrendale, PA, 2005), pp. 1177–1180.

[20] Description of the BT-1 high-resolution neutron powder diffractometer can be found at the NCNR web site (http://www.ncnr.nist.gov).

[21] E. F. Bertaut, J. Appl. Phys. **33**, 1138 (1962); Acta Crystallogr. **A24**, 217 (1968); J. Phys. Colloq. **32**, C1-462 (1971); J. Magn. Magn. Mater. **24**, 267 (1981).

[22] A. Wills, Physica B **276-278**, 680 (2000).

[23] J. Rodriguez-Carvajal, Physica B **192**, 55 (1993).

[24] P. Schobinger-Papamantellos, J. Magn. Magn. Mater. **28**, 97 (1982).

[25] I. P. Semitelou, H. Konguetsof, and J. K. Yakinthos, J. Magn. Magn. Mater. **79**, 131 (1989).

[26] E. M. Levin, V. K. Pecharsky, and K. A. Gschneidner Jr., Phys. Rev. B **62**, R14625 (2000).